International Journal of Mass Spectrometry 274 (2008) 1–7

Contents lists available at ScienceDirect

International Journal of Mass Spectrometry

journal homepage: www.elsevier.com/locate/ijms

Structure and stability of high-spin $Li_{n-1}X$ (n = 2–8, X = Li, Na, and K) clusters

Zhen-Yi Jiang [a,*], Xin-Wei Cao [a], Kuo-Hsing Lee [b,c], San-Yan Chu [c,**]

[a] Institute of Modern Physics, Northwest University, Xian 710069, China
[b] Department of Advanced Fiber Materials and Applications, MCL/ITRI, Hsinchu 30013, Taiwan
[c] Department of Chemistry, National Tsing Hua University, Hsinchu 30013, Taiwan

ARTICLE INFO

Article history:
Received 5 February 2008
Received in revised form 2 April 2008
Accepted 2 April 2008
Available online 10 April 2008

Keywords:
Cluster
Maximum-spin
Structure
Charge distribution
Stability

ABSTRACT

The structures, relative stability and charge distributions in the maximum-spin $^{n+1}Li_{n-1}X$ and $^{n}Li_{n-1}X^{+}$ (n = 2–7, X = Li, Na and K) clusters have been studied with density functional calculations. We predicted the existence of a number of previously unknown cationic isomers. Our results revealed that all high-spin $Li_{n-1}X$ clusters can be derived from capping an X atom over the high-spin Li_{n-1}. Larger heter-atoms favor to occupy outer positions in order to decrease geometrical reconstruction. The high-spin bimetallic clusters tend to holding three-dimensional geometry rather than planar form in low-spin situations whereas smaller ions adopt linear-like form to reduce their repulsive force among atoms. In various high-spin $Li_{n-1}X$ (X = Li, Na and K, n = 2–8) neutral and cationic species, $^{5}Li_3X$ and $^{3}Li_2X^{+}$ are predicted to be of high stability, which can be explained by valence bond theory.

1. Introduction

Clusters are nano-sized materials between isolated molecules and condensed macroscopic states. Some of the fundamental problems which one would like to understand about clusters are their structures, relative stabilities, and their evolutionary regularity as the clusters grow to condensed macroscopic states. Theoretical calculations take an important key role in understanding experimental observations due to lacking of experimentally direct information available on their geometries. The alkali aggregates are among the better known micro-clusters, both experimentally and theoretically. Most of the studies of alkali clusters [1–24] focused on the ground state which is low-spin and bonded by electron pair. Recently the non-pairing alkali clusters [25,26] were probed by experimental photo-association spectroscopy and found to be weakly bound relative to the two separated ground state atoms. According to both molecular orbital and valence bond theories, singlet electron-pair is a fundamental form of bonding in the ground state of closed-shell molecules whereas triplet coupling is associated with a repulsive anti-bonding interaction. This paradigm seems breakdown as one observed the situation on non-pairing electron in Cs_2 ($^3\Sigma_u^+$) dimer. The theoretical studies further showed that their bonding energy rise quite steeply as the high-spin $^{n+1}Li_n$ clusters increase in size, reaching 0.5 eV/atom for $^{13}Li_{12}$ despite the lack of any electron pairs between the atoms [27–33]. These types of clusters are higher in energy than the corresponding lowest-spin states, but stable with respect to isolated lithium atoms. This is quite a surprising result as the triplet state of H_2 is not bound. Owing to the novelty of this non-pairing ferromagnetic-bonding and its occurrence in alkali clusters, it is interest to probe the nature of this bonding and structural characteristics by theoretical means. Until now some geometrical configurations of maximum-spin pure lithium clusters [26–33] have been reported, however, the geometries, charge distributions, and relative stabilities of maximum-spin mixed lithium clusters have not been well understood. Especially, the structures of positively charged mixed lithium clusters may have fully different topological characteristics relative to their neutral species and still remain unclear. So our calculations focus on improving the understanding of the structures and charge distributions of high-spin doped lithium species, which are devoid of electron pairs but nevertheless are strongly bonded.

2. Computational details

Initial geometrical optimizations were performed on high-spin mixed lithium clusters at the B3PW91/6-31G(d) level. The Becke's three-parameter (B3) exchange as well as Perdew and Wang (PW91) correlation [34,35] were used due to their excellent agreements with UCCSD(T) and UQCISD(T) calculations [28,31] on lithium clusters in previous theoretical calculations [29,30].

* Corresponding author. Tel.: +86 29 88303490; fax: +86 29 88302331.
** Corresponding author.
E-mail addresses: jiangzy@nwu.edu.cn (Z.-Y. Jiang), sychu@mx.nthu.edu.tw (S.-Y. Chu).

1387-3806/$ – see front matter © 2008 Elsevier B.V. All rights reserved.
doi:10.1016/j.ijms.2008.04.002

Table 1
Binding energies per atom (BE), basis set superposition per atom (BSSE), zero point energies per atom (ZPE) and corrected binding energies per atom (CBE) (kcal/mol) of all high-spin clusters

Li–Na	BE	BSSE	ZPE	CBE
^{3}LiNa	0.24	0.03	0.04	0.17
^{4}Li$_2$Na	1.77	0.06	0.19	1.52
^{5}Li$_3$Na (Fig. 1a)	5.13	0.10	0.38	4.65
^{6}Li$_4$Na (Fig. 1d)	5.92	0.08	0.41	5.43
^{7}Li$_5$Na (Fig. 2b)	6.38	0.10	0.48	5.80
^{8}Li$_6$Na (Fig. 3a)	7.22	0.10	0.49	6.63
^{9}Li$_7$Na (Fig. 4a)	8.20	0.11	0.53	7.56
^{2}LiNa$^+$	11.27	0.05	0.13	11.09
^{3}Li$_2$Na$^+$	12.99	0.05	0.24	12.70
^{4}Li$_3$Na$^+$ (Fig. 1c)	12.96	0.07	0.30	12.59
^{5}Li$_4$Na$^+$ (Fig. 2a)	12.55	0.05	0.36	12.14
^{6}Li$_5$Na$^+$ (Fig. 2d)	12.56	0.08	0.43	12.05
^{7}Li$_6$Na$^+$ (Fig. 3d)	12.39	0.07	0.44	11.88
^{8}Li$_7$Na$^+$ (Fig. 4a)	12.35	0.09	0.48	11.78
Li-K	**BE**	**BSSE**	**ZPE**	**CBE**
^{3}LiK	0.41	0.01	0.05	0.35
^{4}Li$_2$K	2.13	0.03	0.19	1.91
^{5}Li$_3$K (Fig. 1a)	5.47	0.06	0.37	5.04
^{6}Li$_4$K (Fig. 1d)	6.06	0.07	0.40	5.59
^{7}Li$_5$K (Fig. 2b)	6.70	0.08	0.47	6.15
^{8}Li$_6$K (Fig. 3b)	7.47	0.08	0.47	6.92
^{9}Li$_7$K (Fig. 4a)	8.41	0.09	0.52	7.80
^{2}LiK$^+$	6.14	0.01	0.10	6.03
^{3}Li$_2$K$^+$	8.23	0.02	0.21	8.00
^{4}Li$_3$K$^+$ (Fig. 1c)	8.98	0.03	0.28	8.67
^{5}Li$_4$K$^+$ (Fig. 1e)	9.36	0.06	0.40	8.90
^{6}Li$_5$K$^+$ (Fig. 2d)	9.98	0.06	0.43	9.49
^{7}Li$_6$K$^+$ (Fig. 3d)	10.04	0.06	0.43	9.55
^{8}Li$_7$K$^+$ (Fig. 4a)	10.48	0.07	0.48	9.93

Many different geometrical configurations were tested with a variety of symmetry groups. These isomers were further optimized at B3PW91/6-311G(d) level. After optimizations, partial charges were obtained from Natural Population Analysis (NPA) [36,37]. The NPA solves most of the problems of the Mulliken scheme by construction of a more appropriate set of atomic basis functions, and so the atomic charges from NPA are reliable and usually independent of the basis sets. Frequency analyses were also performed at the final theoretical level to check whether the optimized structures are transition states or true minima on the potential energy surfaces of corresponding clusters. All of the obtained most stable neutral and cationic high-spin clusters were characterized as energy minima without imaginary frequencies. All calculations were carried out using the GAUSSIAN03 program [38].

In all situations, atomic spin densities and natural charges were checked in the output files and it was confirmed that no polarization effects occurred. Moreover the atomic–atomic density was checked, thus confirming the lack of bonding electron pairs (Table 1).

3. Geometrical structures

The lowest-energy geometries of mixed lithium clusters are shown in Figs. 1–4. Bigger and smaller ball represent X and Li atoms, respectively. The numbers inside of the circles in Figs. 1–4 denote the atomic number and mainly used for giving information of bond lengths in Tables 2–4 of Electronic Supporting Information. All reported energetic differences of various isomers in paragraph are based on SCF energy with zero-point energy correction.

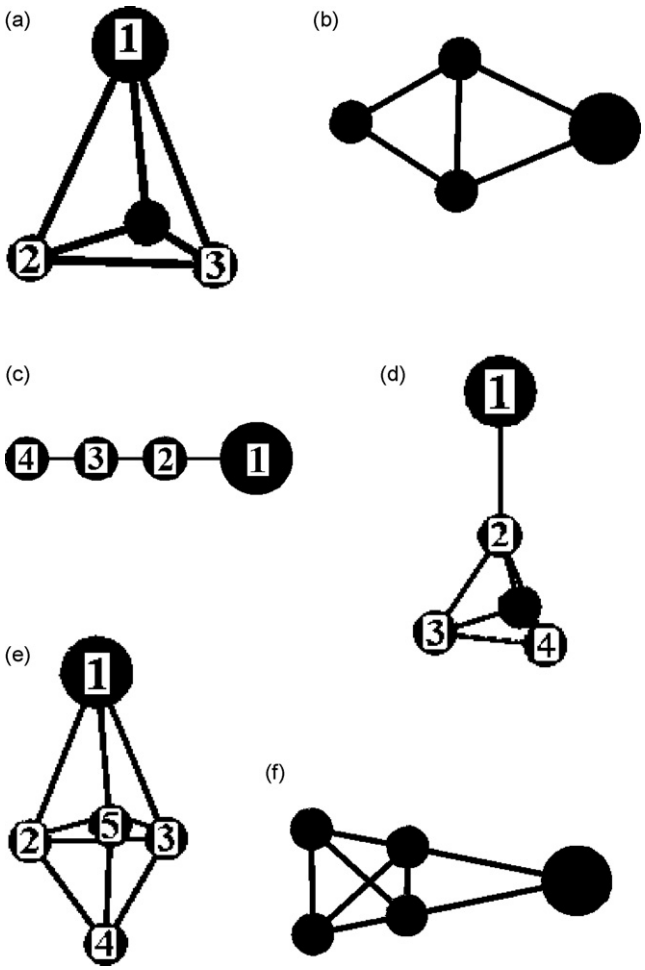

Fig. 1. Low-lying high-spin isomers of (a–c) Li_3X and (d–f) Li_4X clusters.

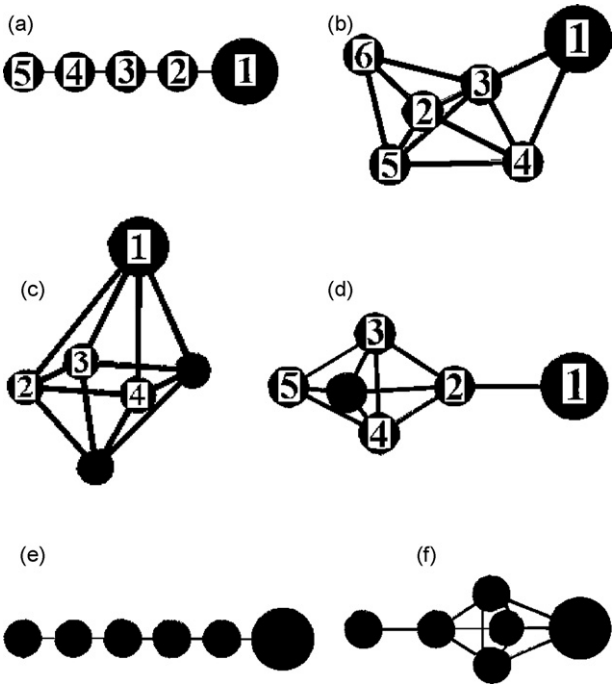

Fig. 2. Low-lying high-spin isomers of (a) Li_4X and (b–f) Li_5X clusters.

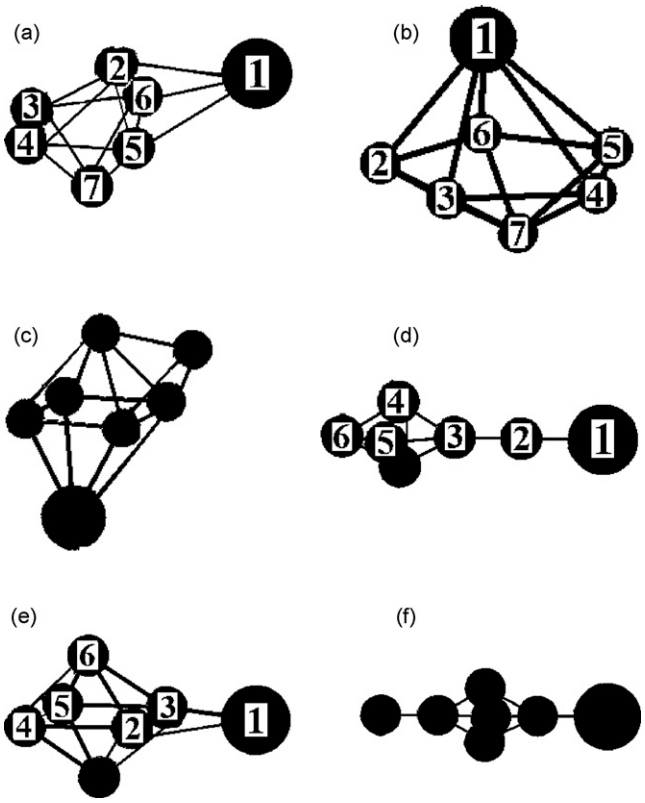

Fig. 3. Low-lying high-spin isomers of (a–f) Li_6X clusters.

3.1. ^3LiX

The smallest mixed lithium clusters are dimers and in the high-spin state (triplet) these species are only weakly bound. Details of the nature of the triplet no-pairing bond can be found in Ref. [28]. Our theoretical binding energies/atom of $^3Li_2$ ($^3\Sigma_u^+$, $D_{\infty h}$), ^{3}LiNa, and ^{3}LiK ($^3\Sigma_g^+$, $C_{\infty v}$) are 0.50, 0.17 and 0.35 kcal/mol, respectively, which are expectably lower than those of corresponding ground state molecules (9.28 for $^1Li_2$, 7.93 for ^{1}LiNa, and 6.80 kcal/mol for ^{1}LiK). At the UQCISD(T,fc)/6-31G*//UMP2(full)/6-31G* level of theory, a binding energy of 0.6 kcal/mol was found [27] and calculations [28] at the UCCSD(T,full)/cc-pVDZ level of theory gave 0.7 kcal/mol for $^3Li_2$. Studies with various theoretical levels [27–32] also further imply our computational method is accurate and reliable. $^3Li_2$, ^{3}LiNa and ^{3}LiK have longer "bond" lengths, hereafter referred to as bond lengths, relative to their low-spin molecules. Previous calculations [37] with Hartree-Fock self-consistent field (HF-SCF) theory showed this no-pairing bonding is not a simple outcome of s–p orbital hybridization which is optimal at the SCF orbital level but rather than a result of essentially covalent bonds, augmented by valence and dynamic electron correlation.

$^2Li_2^+$ ($^2\Sigma_g^+$, $D_{\infty h}$) and ^{2}LiNa$^+$/^{2}LiK$^+$ ($^2\Sigma_g^+$, $C_{\infty v}$) have shorter bond lengths relative to their neutral maximum-spin states. Their binding energies/atom are 14.35 (Li_2^+), 11.09 (LiNa$^+$), and 6.03 kcal/mol (LiK$^+$), respectively, which are much larger than those of corresponding neutral maximum-spin states. They are also larger than those of the corresponding neutral ground state species except the last case. ^{2}LiX$^+$ holds only one valence electron and their larger binding energies can be well explained with larger core/valence interactions relative to the valence/valence interactions [39].

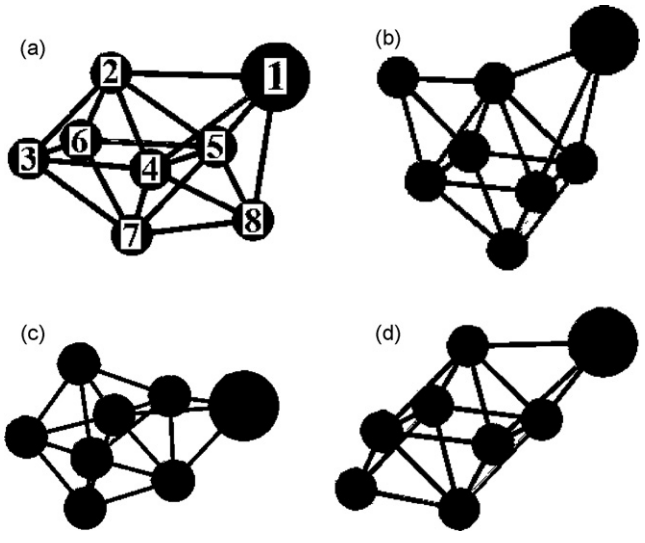

Fig. 4. Low-lying high-spin isomers of (a–d) Li_7X clusters.

3.2. $^4Li_2X$

The lowest-energy state of $^4Li_2X$ (X = Li, Na and K) is triangle configuration ($^4A'$, D_{3h}) for $^4Li_3$ and ($^4B_2$, C_{2v}) for $^4Li_2Na$/$^4Li_2K$, which can be viewed as capping an X atom along the transverse direction of lithium dimer. The distribution of atomic electronic charges in both $^4Li_3$ and $^4Li_2Na$ tends to be even due to smaller difference of the ionization potential, hereafter referred to as IP, between sodium and lithium atoms. Potassium atom holds much more positive charges in $^4Li_2K$ owing to its lower IP.

Another two linear species ($^4\Sigma_u$, $D_{\infty h}$) and ($^4\Sigma$, $C_{\infty v}$) for $^4Li_2Na$/$^4Li_2K$ are local minima with positive frequencies only, but are considerably higher in energy than the triangle by 3.33, 8.23 kcal/mol ($^4Li_2Na$) as well as 4.02, 8.23 kcal/mol ($^4Li_2K$), respectively. Interestingly, the energy of the linear with central heavy atom ($D_{\infty h}$) is lower than that with peripheral heavy atom ($C_{\infty v}$), which differs from our previous results [39] for low-spin mixed lithium clusters. The overturn of energy order may result from smaller repelling interaction between spin-parallel electrons for linear ($D_{\infty h}$) with farther atomic distance.

$^3Li_2X^+$ ions undergo substantial structural changes upon ionization and surprisingly adopt linear form with peripheral heavy atom, which can be considered as capping an X cation along the radial direction of lithium dimer. Compared with $^4Li_2X$ and $^1Li_2X^+$ ion [39] with triangle topology, the significant repulsive interaction in $^3Li_2X^+$ was found to arise from the force between spin-parallel electrons and between positively charged terminal atoms. These make triangle unstable and then the linear with peripheral heavy atom is stabilized due to farther atomic interval. These types of repelling forces unceasingly dominate the cationic geometries up to mixed heptamer as follows. In linear $^3Li_2X^+$, the peripheral atoms have much more positive charges so as to lower repulsive electrostatic force. Based on the reason for IP above mentioned, potassium atom possesses much more positive charges whereas sodium holds nearly the same ones as peripheral lithium atom.

The second triplet mixed trimer ion was found to be linear ($D_{\infty h}$) with central heavy atoms, lying 3.45 ($^3Li_2Na^+$) and 3.77 kcal/mol ($^3Li_2K^+$) relative to their corresponding lowest-energy high-spin ions. The isosceles triangle (C_{2v}) with an imaginary frequency locates at 8.42 ($^3Li_2Na^+$) and 9.48 kcal/mol ($^3Li_2K^+$) higher in energy.

3.3. $^5Li_3X$

The pyramid ($^5A_1$, T_d) for $^5Li_4$ and ($^5A_1$, C_{3v}) for $^5Li_3Na$/$^5Li_3K$ (Fig. 1(a)) can be described as capping an X atom over lithium triangle $^4Li_3$ (D_{3h}). $^5Li_3X$ prefers to adopt three-dimensional geometry relative to the low-spin ground state Li_3X molecules with planar rhombus [39] (Fig. 1(b)).

In the low-spin state the rhombus was predicted to be the lowest energy structure [39] whereas at the quintet spin state this structure ($^5A_2$, C_{2v}) (Fig. 1(b)), lying 8.79 ($^5Li_3Na$) and 8.35 kcal/mol ($^5Li_3K$) higher in energy above their corresponding lowest-energy states, is a first-order saddle point with an imaginary frequency. The imaginary frequency shows its tendency to distort towards pyramid topology. The repulsive Pauli exclusion among four non-pairing electrons results in the destabilization of planar rhombus and then stabilizes the pyramid with higher symmetry and maximum coordination number. This type of pyramid also indicates that the maximum-spin clusters prefer to adopt three-dimensional form and may be applied into other maximum-spin noble metal clusters, i.e., Au_n, in which their ground states often possess planar configurations. The third quintet is a fan-shaped planar ($^5A_2$, C_{2v}) with an imaginary frequency, in which Na/K atom bonds with three lithium atoms on a plane similar to Fig. 1(b), lying 10.30 ($^5Li_3Na$) and 10.87 kcal/mol ($^5Li_3K$) higher in energy. Their vibration direction of the imaginary frequency indicates they try to transform into the pyramid (Fig. 1(a)).

$^4Li_3X^+$ also holds linear form ($^4\Sigma_u$, $D_{\infty h}$) for $^4Li_4^+$ and ($^4\Sigma$, $C_{\infty v}$) for $^4Li_3Na^+$/$^4Li_3K^+$ (Fig. 1(c)) analogous to $^3Li_2X^+$, which also can be considered as capping an X cation over the lowest-energy high-spin linear $^3Li_3^+$ ion. The significant repulsive force between spin-parallel electrons and between positively charged terminal atoms will make pyramid structure destabilization and further transfer into a linear configuration. In linear $^4Li_3X^+$ ions, the peripheral atoms have much more positive charges so as to lower repulsive electrostatic interaction similar to $^3Li_2X^+$. Potassium atom possesses much more positive charges relative to sodium and lithium atoms.

The second quartet mixed cationic state was found to be a triangle with a tail of heavy atom ($^4B_2$, C_{2v}), lying 3.96 ($^4Li_3Na^+$) and 3.96 kcal/mol ($^4Li_3K^+$) relative to their corresponding lowest-energy cationic states. A linear with central heavy atom ($^4\Sigma$, $C_{\infty v}$) holds an imaginary frequency, located at 4.02 ($^4Li_3Na^+$) and 4.90 kcal/mol ($^4Li_3K^+$) higher in energy.

3.4. $^6Li_4X$

A new tower-shaped geometry ($^6A_1$, C_{3v}) for $^6Li_4Na$/$^6Li_4K$ (Fig. 1(d)) is energetically favorable, which can be understood as capping a Na/K atom over an apical atom for $^5Li_4$ pyramid (T_d). For pure sextet lithium pentamer a bipyramid ($^6A_2$, C_{2v}) analogous to Fig. 1(e) was predicted to be lowest-energy configuration, which agrees with previous calculations [29]. The tower-shaped topology (Fig. 1(d)) is the third lowest-energy at B3PW91/6-311G(d) level in pure sextet lithium pentamer, however both Glukhovtsev [27] and Visser [29] have not found this isomer due to their study of neutral high-spin species only.

These followed by two transition states. One is a tower-like conformation ($^6A_2$, C_{2v}) (Fig. 1(f)), derived from capping a Na/K atom against an edge for a Li_4 pyramid (T_d), just lying 0.94 ($^6Li_4Na$) and 0.50 kcal/mol ($^6Li_4K$) higher in energy. Another is a bipyramid ($^6A_1$, C_{3v}) (Fig. 1(e)), lying 1.82 ($^6Li_4Na$) and 0.25 kcal/mol ($^6Li_4K$) higher in energy. We should point out these two isomers for $^6Li_4Na$ and $^6Li_4K$ hold reversal energy order. Their imaginary frequencies in these two species lead to a distortion towards tower-shaped structure (Fig. 1(d)).

$^5Li_5^+$/$^5Li_4Na^+$ also adopts linear form ($^5\Sigma_g$, $D_{\infty h}$) for $^5Li_5^+$ and ($^5\Sigma$, $C_{\infty v}$) for $^5Li_4Na^+$ (Fig. 2(a)), which also can be considered as capping a Li/Na atom over the lowest-energy high-spin linear $^4Li_4^+$ ($^4\Sigma_u$, $D_{\infty h}$) cluster. That significant repulsive force between spin-parallel electrons and between positively charged terminal atoms also dominates the topology in pure and sodium-doped lithium pentamer, however for potassium-doped lithium pentamer the role taken by this repelling force falls down. For $^5Li_4K^+$ the cage-like bipyramid ($^5A_1$, C_{3v}) (Fig. 1(e)) becomes the lowest-energy high-spin cationic state. The reason for structural difference between $^5Li_5$/$^5Li_4Na^+$ and $^5Li_4K^+$ ions results from the gradual fall of repelling force as increase of cluster size. The larger atomic radius of K atom make the geometrical structure of cage-like bipyramid (Fig. 1(e)) of $^5Li_4K^+$ ions to be larger and then the interaction of chemical bonding takes key role in stabilization. It is apparent that strong chemical bonding is work here, rather than weak van der Waals forces [30] due to the delocalization of individual electron.

For $^5Li_4Na^+$ the linear (Fig. 2(a)) is more stable than the bipyramid (Fig. 1(e)) by 3.14 kcal/mol, and contrarily for $^5Li_4K^+$ ions the linear (Fig. 2(a)) lies at just 0.38 kcal/mol higher in energy relative to the bipyramid (Fig. 1(e)). The third sextet cationic ion is the tower-like conformer ($^5A_2$, C_{2v}) (Fig. 1(f)), located at 3.96 ($^5Li_4Na^+$) and 1.19 kcal/mol ($^5Li_4K^+$) higher in energy relative to their corresponding lowest-energy states. Interestingly, the tower-like conformer (Fig. 1(f)) for $^5Li_4K^+$ is a transition state whereas that for $^5Li_4Na^+$ is a local minimum. Its imaginary frequency indicates its tendency to distort towards the cage-shaped topology (Fig. 1(e)), which also supports our prediction on lowest-energy geometrical structure for $^5Li_4K^+$. For tower-like conformer (Fig. 1(f)) of $^5Li_4Na^+$, there exists another local minimum and a nearly degenerate state ($^5A_2$, C_{2v}) (4.08 kcal/mol higher in energy), which is derived from a substitution of a Li at lumbar sites by a Na atom in lithium pentamer bipyramid (D_{3h}).

3.5. $^7Li_5X$

For $^7Li_5Na$/$^7Li_5K$, we found a distorted cage-like geometry (Fig. 2(b)) as lowest-energy conformation ($^7A'$, C_s), which can be described as capping a Na/K atom along vertical direction to atomic surface over the $^6Li_5$ bipyramid (C_{2v}) (Fig. 1(e)). It is also the lowest-energy isomer in the low-spin neutral and cationic Li_5X (X = Na and K) cluster [39]. For heptet pure lithium hexamer this topology cannot obtained a converged optimization in our and Visser's [29] calculations. We basically support Visser's results [29] that the most stable septuplet lithium hexamer is a degenerate pair formed by a rectangular diamond ($^7B_{2u}$, D_{2h}) and a chair (^7B_u, C_{2h}), where both of them are a little similar octahedron (O_h). Both the rectangular diamond and the chair can actually be comprehended as capping a Li atom over the base of $^6Li_5$ bipyramid (C_{2v}). In Visser's calculations the wobbly chair belongs to C_i symmetry. We choose C_{2h} point group rather than C_i due to higher symmetry of C_{2h} and the same total energy they hold.

Another three-dimensional geometry ($^7A_1$, C_{5v}), which is derived from capping a Na/K atom over the surface of lithium cyclic pentamer, was found at 1.13 ($^7Li_5Na$) and 0.44 kcal/mol ($^7Li_5K$) higher in energy, respectively. This followed by a cage-like conformation ($^7A''$, C_s) (Fig. 2(c)) with an imaginary frequency, lying 2.01 ($^7Li_5Na$) and 1.95 kcal/mol ($^7Li_5K$) higher in energy, respectively.

Linear form is no longer lowest-energy for $^6Li_5X^+$. The repulsive force between spin-parallel electrons and between positively charged atoms cannot finally dominate the topology in doped lithium cationic ions anymore. A new bipyramid ($^6A_1$, C_{3v})

(Fig. 2(d)) for $^6Li_5X^+$ (X = Li, Na and K) was energetically favorable state, which can be viewed as capping an X atom over a apical atom of lithium pentamer bipyramid (D_{3h}). A shadow of the repulsive interactions among atoms still worked here can also be observed.

The linear ($^6\Sigma$, $C_{\infty v}$) with a Na/K atom at the top site (Fig. 2(e)) locates at 2.64 ($^6Li_5Na^+$) and 4.21 kcal/mol ($^6Li_5K^+$) above the bipyramid (Fig. 2(d)). Another isomer ($^6A_1$, C_{3v}) (Fig. 2(f)) is predicted to be 2.95 ($^6Li_5Na^+$) and 2.01 kcal/mol ($^6Li_5K^+$) higher in energy. These two isomers for $^6Li_5Na^+$ and $^6Li_5K^+$ ions have reverse energy order and are local minima without any negative frequency.

3.6. $^8Li_6X$

The conformation ($^8A'$, C_s) ($^8Li_6Na$) and ($^8A_1$, C_{3v}) ($^8Li_7$) (Fig. 3(a)) is energetically favored, which can be depicted as capping a Li/Na atom over the rectangular diamond $^7Li_6$. Two isomers ($^8A'$, C_s), (Fig. 3(a) and (b)) for $^8Li_6K$ heptamer, are nearly degenerate, where structure (Fig. 3(b)) ($^8Li_6K$) is more stable by only 0.13 kcal/mol.

Two cage-like configurations ($^8A'$, C_s) are followed. One is the isomer (Fig. 3(c)), derived from a exchange of 1 and 7 atoms in the isomer (Fig. 3(a)), found just at 0.50 ($^7Li_5Na$) and 0.25 kcal/mol ($^7Li_5K$) higher in energy. Another is derived from a exchange of 1 and 2 atoms in the isomer (Fig. 3(a)), lying 0.94 ($^7Li_5Na$) and 0.38 kcal/mol ($^7Li_5K$) higher in energy. These three species actually differ in exotically atomic positions.

There is fully dissimilarity between cationic and neutral topologies. The tower-shaped form (Fig. 3(d)) was still predicted to be most stable configuration ($^7A_1$, C_{3v}) for $^7Li_7^+/^7Li_6X^+$ like the situation in $^6Li_5X^+$ ion, which can be viewed as capping a Li/X atom along the radial direction over the apical atom of $^6Li_6^+$ (C_{3v}) (Fig. 2(d)). However energy difference between the isomer (Fig. 3(d)) and the cage-like geometry ($^7B_2$, C_{2v}) (Fig. 3(e)) is so small (0.06 kcal/mol) and can be regarded as nearly degenerate. The repulsive interactions between spin-parallel electrons and between positively charged atoms still exert a momentous influence on the topologies for pure and sodium-doped lithium cationic ions, however this influence basically vanishes due to increase of atomic intervals at the same time reduction of average positive charges/atom for potassium-doped lithium ions.

For $^7Li_6Na^+$ the topology (Fig. 3(f)) lies 0.63 kcal/mol higher in energy than the lowest-energy bipyramid (Fig. 3(d)), and more stable than the three-dimensional conformation (Fig. 3(e)) by 1.00 kcal/mol. This energy order for $^7Li_6K^+$ isomers is changed. The configuration (Fig. 3(f)) lies 0.69 kcal/mol higher in energy relative to the lowest-energy cage-like $^7Li_6K^+$ ion (Fig. 3(d)).

3.7. $^9Li_7X$

The cage-shaped octamer (^9A, C_1) ($^9Li_7Na/^9Li_7K$) and ($^9B_3$, D_2) ($^9Li_8$) (Fig. 4(a)) was most favorable form, which can be comprehended as capping an X atom over the $^8Li_7$ (C_{3v}) (Fig. 3(a)).

Two isomers both with C_s symmetry at $^9A'$ state (Fig. 4(b) and (c)) locate 2.45 and 3.14 kcal/mol for $^9Li_7Na$ and 2.45 and 2.83 kcal/mol for $^9Li_7K$ higher in energy relative to their corresponding lowest-energy states, respectively.

The repulsive interactions above mentioned cannot anymore take a key role in determine the topologies for doped and pure lithium clusters due to increase of atomic intervals and reduction of average positive charges/atom. So high-spin and low-spin as well as cationic and neutral clusters present a geometrical similarity [39]. The cage-shaped form (Fig. 4(a)) is preserved as the most favorable energetically configuration ($^8A'$, C_s) for $^8Li_7Na^+/^8Li_7K^+$ and ($^8B_2$, D_{2d}) for $^8Li_8^+$.

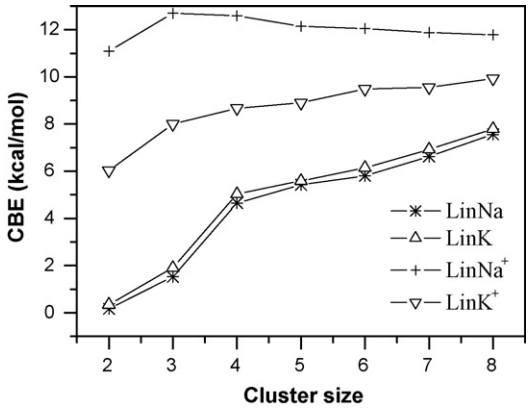

Fig. 5. Corrected binding energies/atom vs. cluster size.

The topology ($^8A_1$, C_{3v}) (Fig. 4(d)) lies 1.26 ($^8Li_7Na^+$) and 0.50 kcal/mol ($^8Li_7K^+$) higher in energy than the lowest-energy cage-like ion (Fig. 4(a)). A new isomer ($^8A'$, C_s) for $^8LiNa^+$, derived from exchange of 1 and 2 atoms in Fig. 4(a), locates 1.38 kcal/mol higher in energy above the lowest energy state. For $^8LiK^+$, the isomer ($^8A''$, C_s) (Fig. 4(b)) is the third state, lying 1.88 kcal/mol higher in energy.

4. Relative stability

4.1. Binding energies

For the optimized structures of the neutral and ionic clusters, binding energies per atom (BE), zero-point energies per atom (ZPE) and basis set superposition error correction [40,41] per atom (BSSE) were calculated and listed in Table 1 due to the existence of weak interactions in high-spin clusters. As can been seen from this table the BSSE lies within 0.11 kcal/mol per atom for the used basis set and has small influence upon BEs. The ZPE increases monotonically from 0.04 to 0.53 kcal/mol as enhance of the cluster size. Our calculations should be useful for future experimental investigations due to no available observations for these clusters at present. The corrected binding energies per atom show a peak value for the Li_3X and Li_2X^+ in Fig. 5, which imply that Li_3X and Li_2X^+ clusters possess higher stability in this series clusters. All BEs for cationic ions are always larger than those for neutral species, which indicates that the influence of repulsive Pauli exclusion among non-pairing electrons on cluster stability is far larger than that of static interactions among electrons.

4.2. Second differences in energy

To describe the relative stabilities of neutral and cationic clusters in this series, the following energy variation of reactions is defined:

$$2(Li_{n-1}X) \rightarrow (Li_nX) + (Li_{n-2}X)$$
$$2(Li_{n-1}X^+) \rightarrow (Li_nX^+) + (Li_{n-2}X^+)$$

We define the second difference in energy as $D2(E_n) = E_{n+1} + E_{n-1} - 2E_n$, so larger second difference in energy should denote higher relative stability of cluster in this series in term of our definition. The pronounced stability for $^5Li_3X$, $^2LiX^+$ and $^3Li_2X^+$ are obvious in Figs. 6 and 7. The special stability of $^2Li_2^+$ and $^2LiNa^+$ has been well understood due to its larger core/valence interactions relative to the valence/valence interactions [39]. According to valence bond theory previous calculations [29–31] elucidated that maximum-spin lithium clusters tend to maximiz-

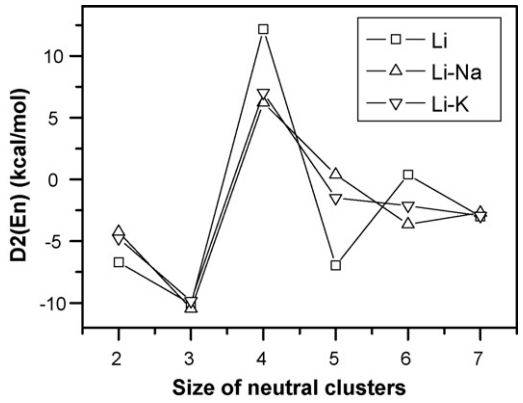

Fig. 6. Second difference in energy of neutral clusters vs. cluster size.

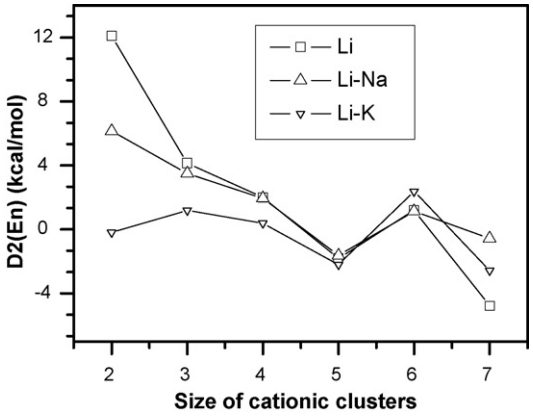

Fig. 7. Second difference in energy of cationic clusters vs. cluster size.

ing the coordination number and create egg-like geometry so as to hold larger total bond dissociation energy of non-pairing clusters, so the super-stability of the pyramid structure for $^{5}Li_3X$ is easily comprehended. $^{7}Li_6$ also has higher value of second difference in energy owing to their composition of two pyramids for rectangular diamond or chair-like isomer. Geometry with lower symmetry always holds some atoms with weaker chemical bonding due to their marginal positions. It is this type of atoms that will lead to be instable for total structure. This situation occurs for $^{7}Li_5Na$ and $^{7}Li_5K$ due to their lower symmetry. $^{3}Li_2X^+$ ions have a linear form and their chemical bonding among three atoms hold stronger interaction relative to larger cationic ions, i.e., $^{4}Li_4X^+$, which lead to be relatively more stable in cationic series except $^{2}Li_2^+$ and $^{2}LiNa^+$. Super-stability of K_5^+ cannot be obtained from our theoretical calculations. The experimental observations [26] on high-spin K_5^+ ion may result from special experimental conditions.

5. Summary

In this work, the structure and stability of the $Li_{n-1}X$ (X = Li, Na and K, n = 2–8) neutral and cationic clusters were studied with B3PW91 at the basis set of 6-311G(d). Our calculations predicted the existence of a number of previously unknown cationic isomers. The gradual evolution of atomic size can be viewed as a sequential capping of an X atom over smaller clusters. Neutral clusters tend to taking three-dimensional geometry rather than planar topology only for high-spin clusters, rather than low-spin clusters. This behavior has been explained and predicted based on the valence bond model [28]. $^{n+1}Li_{n-1}X$ undergo substantial structural changes upon ionization up to 8 atoms of cluster size so as to reduce the repulsive force between spin-parallel electrons and between positively charged atoms. Smaller cationic clusters incline to adopting linear-shaped geometrical structures whereas larger cations (n > 7) hold cage-like topology, which has the same geometrical topology as the low-spin lowest-energy cationic state. Larger heter-atoms prefer to occupy outer positions in order to decrease geometrical reconstruction. In various $Li_{n-1}X$ (X = Li, Na and K, n = 2–8) neutral and cationic species, $^{5}Li_3X$ and $^{3}Li_2X^+$ (X = Li, Na and K) are predicted to be of high stability, which can be explained by valence bond theory.

Acknowledgements

The authors acknowledge the support of National Science Foundation of China under Grant No.10647008 and National Science Council of Taiwan under Grant No. 952113M007034MY2.

Appendix A. Supplementary data

Supplementary data associated with this article can be found, in the online version, at doi:10.1016/j.ijms.2008.04.002.

References

[1] P. Fantucci, J. Koutecký, G. Pacchioni, J. Chem. Phys. 80 (1984) 325.
[2] J.L. Martins, J. Buttet, R. Car, Phys. Rev. B 31 (1985) 1804.
[3] B.K. Rao, P. Jena, Phys. Rev. B 32 (1985) 2058.
[4] I. Boustani, W. Pewestorf, P. Fantucci, V. Bonačić-Koutecký, J. Koutecký, Phys. Rev. B 35 (1987) 9437.
[5] I. Boustani, J. Koutecký, J. Chem. Phys. 88 (1988) 5657.
[6] V. Bonačić-Koutecký, P. Fantucci, J. Koutecký, Phys. Rev. B 37 (1988) 4369.
[7] I. Moullet, J.L. Martins, F. Reuse, J. Buttet, Phys. Rev. Lett. 65 (1990) 476.
[8] T.A. Dahlseid, M.M. Kappes, J.A. Pople, M.A. Ratner, J. Chem. Phys. 96 (1992) 4924.
[9] V. Bonačić-Koutecký, J. Gaus, M.F. Guest, J. Koutecký, J. Chem. Phys. 96 (1992) 4934.
[10] S. Pollack, C.R.C. Wang, T.A. Dahlseid, M.M. Kappes, J. Chem. Phys. 96 (1992) 4918.
[11] R.O. Jones, A.I. Lichtenstein, J. Hutter, J. Chem. Phys. 106 (1997) 4566.
[12] R. Rousseau, D. Marx, Phys. Rev. A 56 (1997) 617.
[13] R. Antoine, D. Rayane, A.R. Allouche, M. Aubert-Frécon, E. Benichou, F.W. Dalby, P. Dugourd, M. Broyer, C. Guet, J. Chem. Phys. 110 (1999) 5568.
[14] P. Calaminici, K. Jug, A.M. Köster, J. Chem. Phys. 111 (1999) 4613.
[15] R. Rousseau, D. Marx, Chem. Eur. J. 6 (2000) 2982.
[16] M. Pecul, M. Jaszuński, P. Jørgensen, Mol. Phys. 98 (2000) 1455.
[17] L. Kronik, I. Vasiliev, M. Jain, J.R. Chelikowsky, J. Chem. Phys. 115 (2001) 4322.
[18] M.D. Deshpande, D.G. Kanhere, I. Vasiliev, R.M. Martin, Phys. Rev. A 65 (2002) 033202.
[19] M.D. Deshpande, D.G. Kanhere, P.V. Panat, I. Vasiliev, R.M. Martin, Phys. Rev. A 65 (2002) 053204.
[20] K.R.S. Chandrakumar, T.K. Ghanty, S.K. Ghosh, J. Chem. Phys. 120 (2004) 6487.
[21] K.R.S. Chandrakumar, T.K. Ghanty, S.K. Ghosh, J. Phys. Chem. A 108 (2004) 6661.
[22] K.R.S. Chandrakumar, T.K. Ghanty, S.K. Ghosh, Int. J. Quantum Chem. 105 (2005) 166.
[23] B. Temelso, C.D. Sherrill, J. Chem. Phys. 122 (2005) 064315.
[24] S.E. Wheeler, H.F. Schaefer III, J. Chem. Phys. 122 (2005) 204328.
[25] A. Fioretti, D. Comparat, A. Crubellier, O. Dulieu, F. Masnou-Seeuws, P. Pillet, Phys. Rev. Lett. 80 (1998) 4402.
[26] C.P. Schulz, P. Claas, D. Schumacher, F. Stienkemeier, Phys. Rev. Lett. 92 (2004) 013401.
[27] M.N. Glukhovtsev, P. von Ragué Schleyer, Isr. J. Chem. 33 (1993) 455.
[28] D. Danovich, W. Wu, S. Shaik, J. Am. Chem. Soc. 121 (1999) 3165.
[29] S.P. De Visser, Y. Alpert, D. Danovich, S. Shaik, J. Phys. Chem. A 104 (2000) 11223.
[30] S.P. De Visser, D. Danovich, W. Wu, S. Shaik, J. Phys. Chem. A 106 (2002) 4961.
[31] S.P. De Visser, D. Danovich, S. Shaik, Phys. Chem. Chem. Phys. 5 (2003) 158.
[32] M.E. Alikhani, S. Shaik, Theor. Chem. Acc. 116 (2006) 390.
[33] S. Hotta, K. Doi, K. Nakamura, A. Tachibana, J. Chem. Phys. 117 (2002) 142.
[34] A.D. Becke, J. Chem. Phys. 98 (1993) 5648.
[35] J.P. Perdew, Y. Wang, Phys. Rev. B 45 (1992) 13244.
[36] A.E. Reed, R.B. Weinstock, F. Weinhold, J. Chem. Phys. 83 (1985) 735.
[37] A.E. Reed, L.A. Curtiss, F. Weinhold, Chem. Rev. 88 (1988) 899.
[38] M.J. Frisch, G.W. Trucks, H.B. Schlegel, G.E. Scuseria, M.A. Robb, J.R. Cheeseman, J.A. Montgomery Jr., T. Vreven, K.N. Kudin, J.C. Burant, J.M. Millam, S.S. Iyengar, J. Tomasi, V. Barone, B. Mennucci, M. Cossi, G. Scalmani, N. Rega, G.A. Petersson, H. Nakatsuji, M. Hada, M. Ehara, K. Toyota, R. Fukuta, J. Hasegawa, M. Ishida, T. Nakajima, Y. Honda, O. Kitao, H. Nakai, M. Klene, X. Au, J.E. Knox, H.P. Hratchian,

J.B. Cross, C. Adamo, J. Jaramillo, R. Gomperts, R.E. Stratmann, O. Yazyev, A.J. Austin, R. Cammi, C. Pomelli, J.W. Ochterski, P.Y. Ayala, K. Morokuma, G.A. Voth, P. Salvador, J.J. Dannenberg, V.G. Zakrzewski, S. Dapprich, A.D. Daniels, M.C. Strain, O. Farkas, D.K. Malick, A.D. Rabuck, K. Raghavachari, J.B. Foresman, J.V. Ortiz, Q. Cui, A.G. Baboul, S. Clifford, J. Cioslowski, B.B. Stefanov, G. Auu, A. Auashenko, P. Piskorz, I. Komaromi, R.L. Martin, D.J. Fox, T. Keith, M.A. AI-Laham, C.Y. Peng, A. Nanayakkara, M. Challacombe, P.M.W. Gill, B. Johnson, W. Chen, M.W. Wong, C. Gonzalez, J.A. Pople, GAUSSIAN 03, Revision A. 1, Gaussian Inc., Pittsburgh, PA, 2003.
[39] Z.Y. Jiang, K.H. Lee, S.T. Li, S.Y. Chu, Int. J. Mass Spectrom. 253 (2006) 104.
[40] S. Simon, M. Duran, J.J. Dannenberg, J. Chem. Phys. 105 (1996) 11024.
[41] S.F. Boys, F. Bernardi, Mol. Phys. 19 (1970) 553.